

Long-Term Stable, Low-Temperature Remote Silicate Phosphor Thick Films Printed on a Glass Substrate

Jun Sik Kim,^{†,‡} Oh Hyeon Kwon,[†] Jin Woo Jang,[†] Sung Hyun Lee,[‡] Sung Jun Han,[‡] Joo Hong Lee,[‡] and Yong Soo Cho^{*,†}

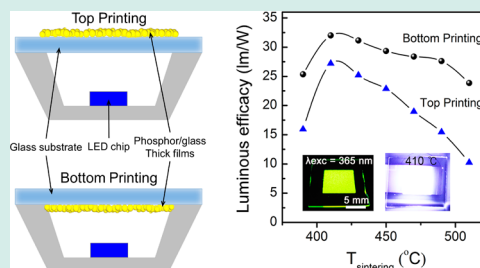
[†]Department of Materials Science & Engineering, Yonsei University, Seoul 120-749, Korea

[‡]R&D Center, LG Display Co., Ltd., Gyeonggi-do 413-811, Korea

Supporting Information

ABSTRACT: A critical step in providing better phosphor solution for white light emitting diode (LED) is to utilize inexpensive silicate phosphors with strong thermal stability. Here, we demonstrate yellow silicate phosphor-embedded glass thick films with a high luminous efficacy of ~ 32 lm/W at 200 mA as a nonconventional remote-phosphor approach. The simple screen-printing process of a paste consisting of $(\text{Ba,Sr,Ca})_2\text{SiO}_4:\text{Eu}^{2+}$ phosphor and a low softening point glass creates a planar remote structure on a regular soda lime silicate glass with controllable film thickness and location (top vs bottom) of the phosphor layer. The glass matrix provides promising densification and adhesion with the substrate at the optimal low temperature of 410 °C, with the long-term stability in luminous efficacy over 500 h of operation. The proposed phosphor structure has important implications to overcome current limitations as phosphors.

KEYWORDS: light-emitting diodes, remote phosphor, silicates, printing, luminescence



INTRODUCTION

The combination of a blue UV (ultraviolet) emitter with a phosphor-embedded resin converter has been a practical solution for generating a high efficiency white light-emitting diode (LED).^{1–4} One issue with the current LED structure lies in that the silicon resin encapsulant causes deterioration in the phosphor due to thermal reaction generated upon LED operation over an extended period of time.^{5,6} It results in the serious degradation of LED performance by accompanying the color change of phosphor resin into yellow. One proposed solution is to change the device structure by separating the phosphor converter from the blue chip to avoid direct contact between them, which corresponds to the remote-phosphor approach.^{7–9} Various attempts to improve the remote phosphor have focused on optimizing the LED performance by developing proper phosphor layers with adjusted composition.^{10–12}

This work introduces a screen-printing process for a nonconventional remote phosphor layer containing low temperature silicates phosphors on a regular soda lime silicate (SLS) glass substrate. This printing approach differs from the known remote phosphor approach incorporating a high temperature-produced pellet that contains a considerable amount of expensive phosphor powder. There have been recent reports on the printing process of phosphors but they are limited to the use of expensive yttrium aluminum garnet (YAG):Ce phosphors fired at high temperatures greater than 700 °C.^{13,14} To use the regular SLS glass substrate, firing temperature needs to be lower than 530 °C. Otherwise, severe

warping of the glass substrate happens as a result of firing at a higher temperature. This low temperature process enabled by an appropriate choice of glass frit allows the use of inexpensive yellow silicate phosphors, $\text{M}_2\text{SiO}_4:\text{Eu}^{2+}$ ($\text{M} = \text{Ca}, \text{Sr}, \text{Ba}$). The silicate phosphor is known to have higher potentials than the other typical phosphors including yttrium aluminum garnet (YAG):Ce, $\text{Ca}_9(\text{Si,Al})_{12}(\text{O,N})_{12}:\text{Eu}^{2+}$, $\beta\text{-SiAlON}:\text{Eu}^{2+}$, and $\text{CaAlSiN}_4:\text{Eu}^{2+}$ from the higher luminescence efficacy, no obstacle of commercial utilization and cost savings.^{15–18} On the other hand, the silicates phosphors are limitedly considered because they are more susceptible to the thermal degradation of luminescent properties with structural changes than the other phosphors.^{15,16}

This work demonstrates for the first time the successful screen-printing of a phosphor thick film on glass substrate, which consists of silicate phosphor powder with a low temperature softening glass frit. The phosphor thick films positioned on the top or bottom of the substrate are compared. Luminescent properties of the LED device with different firing temperatures and over a long-term operation are investigated to suggest the potential of this printing process as another practical solution for white LED.

Received: October 31, 2014

Revised: February 1, 2015

Published: March 11, 2015

RESULTS AND DISCUSSION

Figure 1 presents the schematics of the remote phosphor structure consisting of screen-printed phosphor thick films on

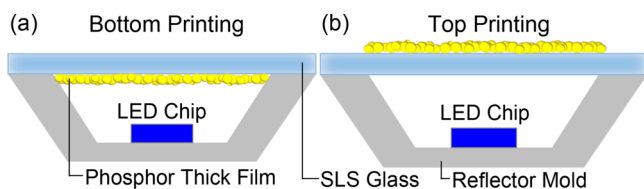


Figure 1. Schematic illustrations of white LED structures consisting of phosphor-embedded glass thick films printed on the (a) bottom and (b) top sides of SLS glass substrate.

the top or bottom side of the SLS glass substrate. There have been no comparative reports regarding the effects of the position of the remote phosphor on luminescence properties. The printing process generates phosphor thick films on the glass substrate with controllable thickness of a few to tens μm level. Here, the optimal fired thickness was $\sim 15 \mu\text{m}$ in terms of luminous efficacy as demonstrated in the plots of luminous efficacy as a function of film thickness with the cross-sectional images in Figure 1S of the Supporting Information.

Figure 2a shows the examples of XRD patterns of $(\text{Ba,Sr,Ca})_2\text{SiO}_4:\text{Eu}^{2+}$ phosphor thick films fired at 410 and

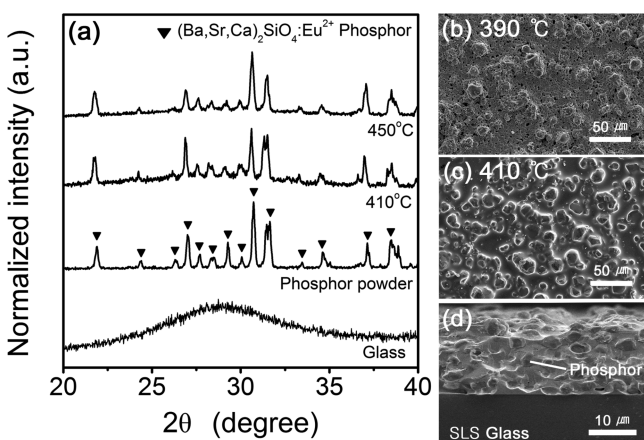


Figure 2. (a) XRD patterns of the phosphor layer fired at 410 and 450 $^{\circ}\text{C}$. For comparison, XRD patterns of phosphor and glass alone are included. Surface SEM images of the phosphor thick films fired at (b) 390 and (c) 410 $^{\circ}\text{C}$. The panel d image corresponds to the cross section of the thick film fired at 410 $^{\circ}\text{C}$.

450 $^{\circ}\text{C}$. For comparison, the patterns of the phosphor powder and Bi silicate glass frit were included. The patterns fired at 410 and 450 $^{\circ}\text{C}$ match well with that of phosphor, indicating that the phosphor is chemically stable with the glass frit upon firing. It is important to maintain the chemical inertness of phosphors with glass at high temperatures since the unwanted diffusion or substitution of elements can change the chemistry of phosphors or induce the crystallization of glass.^{18,19}

Selected SEM images of the printed phosphor layer fired at 390 and 410 $^{\circ}\text{C}$ are seen in Figure 2b and c. The remarkable degree of densification seems to happen already via viscous flow of the glass frit at the low temperature of 390 $^{\circ}\text{C}$, with the remaining enclosed pores dispersed uniformly throughout the film surface. Note that the softening point of the glass frit is $\sim 385 \text{ }^{\circ}\text{C}$. An increase in temperature to 410 $^{\circ}\text{C}$ was enough to

generate nearly full densification. For better visualization on the progress of densification, enlarged surface images of the samples fired at different temperatures were included as Supporting Information Figure S2. Well-dispersed phosphor particles are evident on the surface microstructure. The particles on the surface were confirmed as phosphor particles as shown in the elemental EDS mapping of Supporting Information Figures S3 and S4. The cross-sectional image at 410 $^{\circ}\text{C}$ in Figure 2d confirms the phosphor particles well-embedded in the glass matrix. As the densification of the thick film becomes almost complete, the phosphor particles are likely to protrude from the surface with a substantial reduction in thickness. The smooth interface between glass matrix and phosphor particles suggests very good wettability of the melted glass on the phosphor particles at elevated temperatures. The printed phosphor layer was rough with an estimated surface roughness of $\sim 0.73 \mu\text{m}$ and a film thickness of $\sim 15 \mu\text{m}$, although its thickness is controllable by adjusting the number of printing. For the optimal performance as a phosphor, a proper thickness with desirable roughness is preferred since the light emitted from a LED chip needs to be excited effectively by the phosphor layer without the loss of photons by reflection or absorption on the neighboring or surface phosphors. The adhesion between the thick film and glass substrate is expected to be excellent since the glass frit in the thick film participates primarily in bonding with the glass substrate upon firing. The simple pencil adhesion test could not quantify the level of adhesion for the thick films fired above 410 $^{\circ}\text{C}$ since they surpassed the highest standard of the evaluation.

Photoluminescence (PL) spectra of the phosphor layer fired at different firing temperatures are shown in Figure 3. A distinguishable broad emission band in the range of 470–740 nm was found regardless of firing temperature, which was obtained by applying a UV light source with an excitation spectrum at $\lambda_{\text{exc}} = 365 \text{ nm}$. The intense band is known to originate from the 5d–4f transition of Eu^{2+} ions because of the

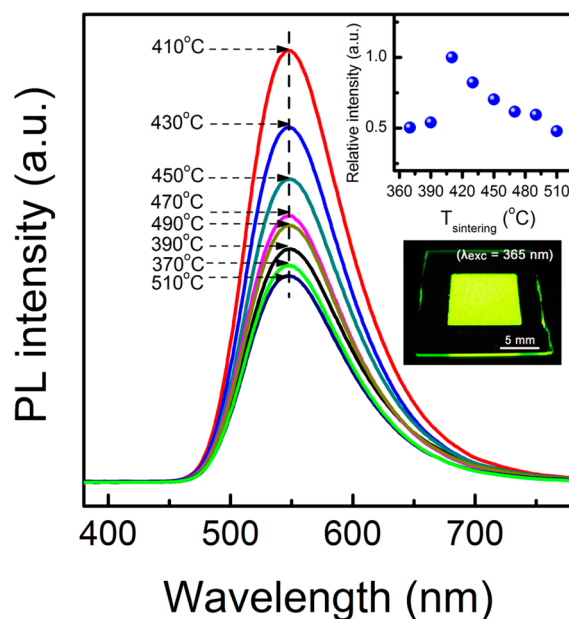


Figure 3. PL spectra of the phosphor layer fired at different temperatures. As insets, the variation in peak intensity at $\sim 547 \text{ nm}$ relative to that of 410 $^{\circ}\text{C}$ with firing temperature is shown with an actual example of yellow emission from the printed phosphor layer.

strong coupling of the 5d electrons with host lattices.^{20,21} The intensity of the band depends on the firing temperature of the phosphor layer, which shows the maximum intensity at 410 °C and then the substantial decreases as firing temperature increases up to 510 °C. The decreasing trend of the emission intensity at temperature above 410 °C was expressed with the variation of peak intensity at 547 nm, which was normalized to the maximum value at 410 °C as represented as an inset of Figure 3. The peak intensity at 547 nm corresponds to the expected yellow emission of the silicate phosphors used here. Another inset of the actual sample fired at 410 °C confirms the intense yellow emission as a result of the 365 nm excitation.

XPS spectra were investigated to understand how luminance characteristics varied with firing temperature. All samples revealed photoelectron peaks corresponding to Bi 5d, Sr 3d, Sr 3p, Bi 4d, Bi 4p, Ba 3d, Zn 2p, and Eu 3d5 emissions (Supporting Information Figure S5). Figure 4 shows the XPS

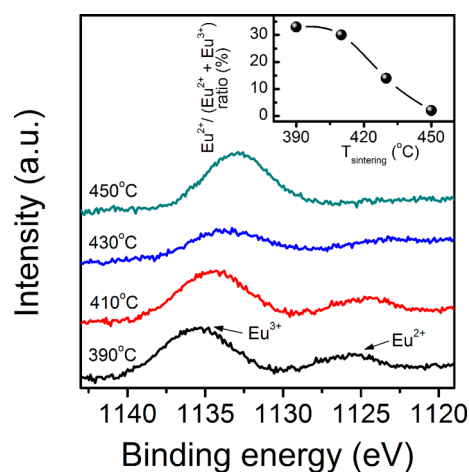


Figure 4. XPS spectra of the phosphor thick films fired at 390, 410, 430, and 450 °C. The variation of the $\text{Eu}^{2+}/(\text{Eu}^{2+} + \text{Eu}^{3+})$ ratio with firing temperature is shown as an inset.

spectra only in the binding energy range of 1120–1140 eV, corresponding to the Eu 3d5 core level with identifiable Eu^{2+} and Eu^{3+} peaks. For clear visualization of the relative peak variation, the $\text{Eu}^{2+}/(\text{Eu}^{2+} + \text{Eu}^{3+})$ ratio was plotted as a function of firing temperature as shown in the inset of Figure 4. The ratio decreases distinctively at temperatures above 410 °C. The result is directly related to the observed luminance degradation at higher temperatures than 410 °C in the PL spectra of Figure 3, which is attributed to thermal degradation with the change in the $\text{Eu}^{2+}/(\text{Eu}^{2+} + \text{Eu}^{3+})$ ratio.^{22,23} The decrease in the relative ratio of Eu^{2+} to Eu^{3+} has been understood by the oxidation mechanism in phosphors.^{22–25} The gaseous oxygen atom adsorbed on the phosphor surface is responsible for the decrease of Eu^{2+} ions by the electronic transfer between the oxygen atom and Eu^{2+} ion. This reaction ultimately results in the transition into Eu^{3+} ions at elevated temperatures by lattice diffusion. Our result matches very well with the reported reduction in the concentration of Eu^{2+} ions in the $\text{BaMgAl}_{10}\text{O}_{17}$ phosphor above ~ 400 °C.²⁵

The luminous performance of the phosphor layers was characterized by exciting the LED samples using a blue diode with $\lambda_{\text{exc}} = 443$ nm. Figure 5a shows the variation in luminous efficacy as a function of firing temperature in the bottom printing. Actual emitted samples of the white light conversion

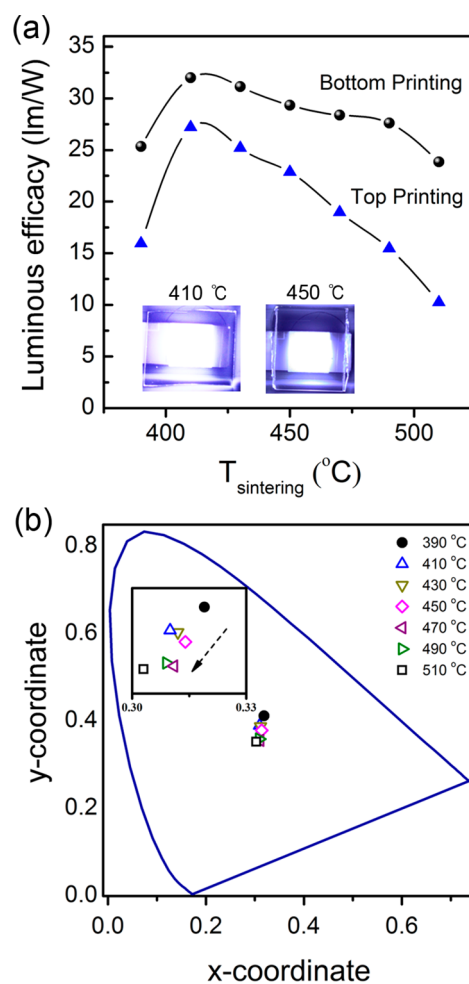


Figure 5. (a) Changes in luminous efficacy of the phosphor thick film device as a function of firing temperature in the bottom and top printing cases, with actual samples excited at 443 nm, and (b) their resultant CIE color coordinates.

for the phosphor layers fired at 410 and 450 °C are seen as insets. The luminous efficacy of the phosphor layer was obtained by the simple relation of $\eta = L/P_{\text{input}}$ where L is the luminous flux (lumens) and P_{input} is the input power of the blue chip. The luminous efficacy was the maximum as ~ 32 lm/W at 410 °C and then decreased gradually at higher temperatures. The varying tendency of the efficacy matches well with that of PL intensity. Since the absolute value of the luminous efficacy depends on the choice of blue chip, only the varying tendency with respect to temperature may be meaningful here.

It should be mentioned that a lower luminous efficacy value of ~ 27.2 lm/W was obtained at 410 °C when the printed phosphor was applied to the top side of the substrate. The higher luminance value in the bottom printing is believed due to the lack of photon absorption by the glass substrate itself prior to the excitation of phosphors. The light intensity is reduced when the emitted photons from the blue chip pass through the glass substrate. The hypothesis was confirmed by observing strong absorption peaks in the range of 380–480 nm in the UV–vis spectrum of the glass substrate alone (Supporting Information Figure S6). It indicates that a portion of the photon energy is absorbed when the light passes through the glass substrate.

Figure 5b shows a Commission Internationale de l'Eclairage (CIE) chromaticity diagram for the phosphor thick films fired at different temperature in the case of the bottom printing, which was obtained under the blue LED excitation. As expected, the results are highly dependent on firing temperature. The coordinates (0.319, 0.412) obtained at 390 °C shifted to the blue region with increasing temperature up to 510 °C. This color coordinate (x , y) shift is believed to be a result of the decreased yellow emission intensity in the PL spectra because of the decreased concentration of Eu^{2+} at higher temperatures.⁹ All samples had correlated color temperatures (CCT) ranging from 6295 to 6812 K, which correspond to the true daylight CCT of about 6500 K.²⁶

The long-term stability of the printed phosphor thick film was estimated in the standard condition of 85 °C and 85 RH%. Figure 6 shows the changes of luminous efficacy with aging for

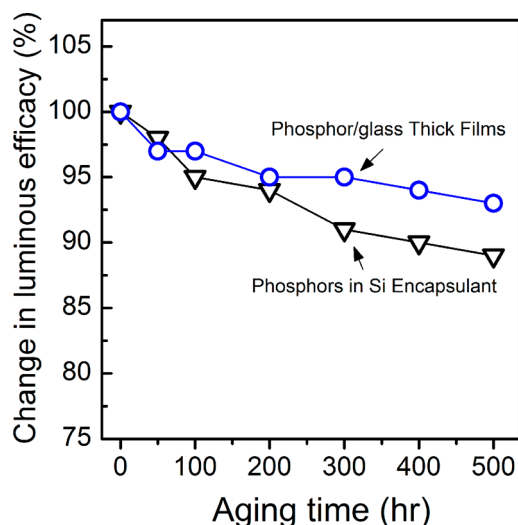


Figure 6. Change in luminous efficacy of the phosphor thick film device over operation time of up to 500 h, compared with the conventional Si resin silicate phosphor sample.

up to 500 h as expressed as the percentage change from the initial value at zero time. The values were obtained for the bottom-printed samples fired at 410 °C. For comparison, the corresponding performance of the identical phosphors encapsulated in a common Si resin was also evaluated. The printed phosphors demonstrate less degradation over the course of the test as compared to the typical Si resin-treated phosphors. As an example, the printed phosphors show ~7% degradation while the phosphors in Si resin exhibit ~12% degradation after 500 h. This result indicates that the glass matrix leads to a higher thermal stability associated with less color change and minimal structural damages in phosphors. Glass usually has a higher bonding strength than resin and is capable of producing less internal stress due to its higher thermal conductivity and lower thermal expansion compared to the resin.²⁷

CONCLUSIONS

Silicate phosphor/glass thick film screen-printed on a SLS substrate demonstrates the potential as a remote phosphor with high luminescence performance when excited by a commercial blue LED. The PL emission intensity of the phosphor film at ~547 nm depends on firing temperature, the level of porosity,

the ratio of $\text{Eu}^{2+}/(\text{Eu}^{2+} + \text{Eu}^{3+})$ and optical transmittance. The firing temperature is limited to ~410 °C because of thermal degradation of the phosphor as confirmed by the lowered luminescence efficacy and the promoted oxidation of Eu^{2+} . The bottom printing of the phosphors is beneficial for minimizing the loss of emitted light. The long-term stability of the printed thick film phosphor is another advantage over the common Si resin approach for white LEDs.

EXPERIMENTAL PROCEDURES

A yellow silicate phosphor $(\text{Ba,Sr,Ca})_2\text{SiO}_4:\text{Eu}^{2+}$ (PA556, Force4 Co., Korea) was selected to form a composite-type phosphor layer with dispersion of the phosphor particles within a glass matrix. A commercially available $\text{Bi}_2\text{O}_3\text{-ZnO-B}_2\text{O}_3$ glass frit (BSP718, DAION Co., Incheon, Korea) with a softening point of ~385 °C and an average particle size of ~2.7 μm was used. The relative ratio of phosphor to glass frit was fixed at 40 wt %.

Viscous ink paste was prepared by admixing the glass frit and silicate phosphor with an organic vehicle composed of 7.4 vol % ethyl cellulose (Kanto Chemical Co., Ltd., Tokyo, Japan), 66.2 vol % α -terpineol (90%, Aldrich, Milwaukee, WI, U.S.A.) and 26.4 vol % lauric acid (98%, Aldrich, Milwaukee, WI, U.S.A.) at 1400 rpm for ~6 min by using a paste mixer. The organic vehicle was separately prepared at ~80 °C for 10 h to become a complete viscous mixture. The resultant paste with a viscosity of ~150 cps was printed 3 times using a 250 mesh screen on a common soda lime silicate (SLS) glass substrate by manual operation to obtain a dried film thickness of ~30 μm . The pattern size was 10 mm \times 10 mm. The printed paste was dried at 120 °C for 1 h and then fired at a temperature between 370 and 510 °C for 30 min.

Phase evolution was analyzed using an X-ray diffractometer (XRD Max-2500, Rigaku, Japan). Surface and cross-sectional microstructures of the phosphor thick film were observed by field emission scanning electron microscopy (FESEM JEOL, JSM-5400, USA). Photoluminescence (PL) spectra of the fired phosphor layers were measured using a fluorescence spectrophotometer (F-7000, Hitachi, Japan) with a Xe lamp at room temperature. Valence states of the ions present in the phosphor films were analyzed by X-ray photoelectron spectroscopy (XPS K-alpha, Thermo U.K.). Luminous efficacy was obtained by an integrating sphere system (ISP 1000, Instrument systems, Germany). The Commission Internationale de l'Eclairage (CIE) chromaticity coordinate was measured in a 1° measuring view field using a colorimeter (PR-650, Photo research, USA) with a 443 nm blue diode as an excitation source.

ASSOCIATED CONTENT

Supporting Information

Thickness dependence of the luminous efficacy, surface SEM images with higher magnification, Elemental mapping of thick film microstructures, and additional information. This material is available free of charge via the Internet at <http://pubs.acs.org>.

AUTHOR INFORMATION

Corresponding Author

*Tel: 82-2-2123-5848. E-mail: ycho@yonsei.ac.kr.

Notes

The authors declare no competing financial interest.

ACKNOWLEDGMENTS

This work was supported by a research grant (NRF-2013R1A2A2A01016711) funded by the National Research Foundation of Korea.

REFERENCES

- (1) Nakamura, S.; Mukai, T.; Senoh, M. Candela-Class High-Brightness InGaN/AlGaIn Double-Heterostructure Blue-Light-Emitting Diodes. *Appl. Phys. Lett.* **1994**, *64*, 1687–1689.
- (2) Chen, L.; Chen, K.; Lin, C.; Chu, C.; Hu, S.; Lee, M.; Liu, R. Combinatorial Approach to the Development of a Single Mass $\text{YVO}_4:\text{Bi}^{3+}$, Eu^{3+} Phosphor with Red and Green Dual Colors for High Color Rendering White Light-Emitting Diodes. *J. Comb. Chem.* **2010**, *12*, 587–594.
- (3) Krames, M. R.; Shchekin, O. B.; Mueller-Mach, G. O.; Zhou, L.; Harbers, G.; Craford, M. G. Status and Future of High-Power Light-Emitting Diodes for Solid-State Lighting. *J. Dispersion Sci. Technol.* **2007**, *3*, 160–175.
- (4) Chen, L.; Luo, A.; Zhang, Y.; Liu, F.; Jiang, Y.; Xu, Q.; Chen, X.; Hu, Q.; Chen, S.; Chen, K.; Kuo, H. Optimization of the Single-Phased White Phosphor of $\text{Li}_2\text{SrSiO}_4:\text{Eu}^{2+}, \text{Ce}^{3+}$ for Light-Emitting Diodes by Using the Combinatorial Approach Assisted with the Taguchi Method. *ACS Comb. Sci.* **2012**, *14*, 636–644.
- (5) Yanagisawa, T.; Kojima, T. Long-Term Accelerated Current Operation of White Light-Emitting Diodes. *J. Lumin.* **2005**, *114*, 39–42.
- (6) Kim, J. P.; Song, S. B. Protective Sol–Gel Coating on Silicate Phosphor Used in Light Emitting Diodes. *Appl. Surf. Sci.* **2011**, *257*, 2159–2163.
- (7) Allen, S. C.; Steckl, A. J. A Nearly Ideal Phosphor-Converted White Light-Emitting Diode. *Appl. Phys. Lett.* **2008**, *92*, No. 143309.
- (8) Nakanishi, T.; Tanabe, S. Novel Eu^{2+} -Activated Glass Ceramics Precipitated With Green and Red Phosphors for High-Power White LED. *IEEE J. Sel. Top. Quantum Electron.* **2009**, *15*, 1171–1176.
- (9) Luo, H.; Kim, J. K.; Xi, Y. A.; Schubert, E. F. Trapped Whispering-Gallery Optical Modes in White Light-Emitting Diode Lamps with Remote Phosphor. *Appl. Phys. Lett.* **2006**, *89*, No. 041125.
- (10) Lin, M. T.; Ying, S. P.; Lin, M. Y.; Tai, K. Y.; Tai, S. C.; Liu, C. H.; Chen, J. C.; Sun, C. C. Ring Remote Phosphor Structure for Phosphor-Converted White LEDs. *IEEE Photonics Technol. Lett.* **2010**, *22*, 574–576.
- (11) Luo, H.; Kim, J. K.; Schubert, E. F.; Cho, J. H.; Sone, C. S.; Park, Y. J. Analysis of High-Power Packages for Phosphor-Based White-Light-Emitting Diodes. *Appl. Phys. Lett.* **2005**, *86*, No. 243505.
- (12) Liu, Z.; Liu, S.; Wang, K.; Luo, X. Optical Analysis of Color Distribution in White LEDs with Various Packaging Methods. *IEEE Photonics Technol. Lett.* **2008**, *20*, 2027–2029.
- (13) Burgin, J.; Jubera, V.; Debeda, H.; Glorieux, B.; Garcia, A.; Lucat, C. Screen-Printed Phosphor Coatings for White LED Emission. *J. Mater. Sci.* **2011**, *46*, 2235–2241.
- (14) Yang, L.; Chen, M.; Lv, Z.; Wang, S.; Liu, X.; Liu, S. Preparation of a YAG:Ce Phosphor Glass by Screen-Printing Technology and Its Application in LED Packaging. *Opt. Lett.* **2013**, *38*, 2240–2243.
- (15) Kim, J. S.; Park, Y. H.; Park, H. L. Temperature-Dependent Emission Spectra of $\text{M}_2\text{SiO}_4:\text{Eu}^{2+}$ ($\text{M} = \text{Ca}, \text{Sr}, \text{Ba}$) Phosphors for Green and Greenish white LEDs. *Solid State Commun.* **2005**, *133*, 445–448.
- (16) Hsu, D.; Skinner, L. Nonperturbative Theory of Temperature-Dependent Optical Dephasing in Crystals. *J. Chem. Phys.* **1984**, *81*, 5471.
- (17) Lee, S.; Huang, C.; Chan, T.; Chen, T. New Ce^{+3} -Activated Triosilicate Phosphor for LED Lighting-Synthesis, Luminescence Studies, and Applications. *ACS Appl. Mater. Interface* **2014**, *6*, 7260–7267.
- (18) Kim, J. S.; Jeon, P. E.; Choi, J. C.; Park, H. L. Emission Color Variation of $\text{M}_2\text{SiO}_4:\text{Eu}^{2+}$ ($\text{M} = \text{Ba}, \text{Sr}, \text{Ca}$) Phosphors for Light-Emitting Diode. *Solid State Commun.* **2005**, *133*, 187–190.
- (19) Kim, B. S.; Lim, E. S.; Lee, J. H.; Kim, J. J. Effect of Structure Change On Thermal and Dielectric Characteristics in Low-Temperature Firing $\text{Bi}_2\text{O}_3\text{--ZnO--B}_2\text{O}_3$ Glasses. *J. Mater. Sci.* **2007**, *42*, 4260–4264.
- (20) Nazarov, M.; Tsukerblat, B.; Noh, D. Y. Electron-Vibrational Interaction in 4f–5d Optical Transitions Ba, Ca, Sr Thiogallates Doped with Eu^{2+} Ions. *J. Lumin.* **2008**, *128*, 1533–1540.
- (21) Kobayashi, T.; Mroczkowski, S.; Owen, J. F. Fluorescence Lifetime and Quantum Efficiency for 5d \rightarrow 4f Transitions in Eu^{2+} Doped Chloride and Fluoride Crystals. *J. Lumin.* **1980**, *21*, 247–257.
- (22) Oshio, S.; Matsuoka, T.; Tanaka, S.; Kobayashi, H. Mechanism of Luminance Decrease in $\text{BaMgAl}_{10}\text{O}_{17}:\text{Eu}^{2+}$ Phosphor by Oxidation. *J. Electrochem. Soc.* **1998**, *145*, 3903–3907.
- (23) Pawar, A. U.; Jadhav, A. P.; Pal, U.; Kim, B. K.; Kang, Y. S. Blue and Red Dual Emission Nanophosphor $\text{CaMgSi}_2\text{O}_6:\text{Eu}^{2+}$: Crystal Structure and Electronic Configuration. *J. Lumin.* **2012**, *132*, 659–664.
- (24) Im, W. B.; Kang, J. H.; Lee, D. C.; Lee, S.; Jeon, D. Y.; Kang, Y. C.; Jung, K. Y. Origin of PL Intensity Increase of $\text{CaMgSi}_2\text{O}_6:\text{Eu}^{2+}$ Phosphor after Baking Process for PDPs Application. *Solid State Commun.* **2005**, *133*, 197–201.
- (25) Bizarri, G.; Moine, B. On $\text{BaMgAl}_{10}\text{O}_{17}:\text{Eu}^{2+}$ Phosphors Degradation Mechanism: Thermal Treatment Effects. *J. Lumin.* **2005**, *113*, 199–213.
- (26) Daniel, A.; Steigerwald, J. C.; Bhat, D. C.; Robert, M. F. Illumination with Solid State Lighting Technology. *IEEE J. Sel. Top. Quantum Electron.* **2002**, *8*, 310–320.
- (27) Wang, J.; Tsai, C. C.; Cheng, W. C.; Chen, M. H.; Chung, C. H.; Cheng, W. H. High Thermal Stability of Phosphor-Converted White Light-Emitting Diodes Employing Ce:YAG-Doped Glass. *IEEE J. Sel. Top. Quantum Electron.* **2011**, *17*, 741–746.